PHYSICAL REVIEW B **92**, 041303(R) (2015)

Magnetoplasma excitations of two-dimensional anisotropic heavy fermions in AlAs quantum wells

V. M. Muravev,[1] A. R. Khisameeva,[1,2] V. N. Belyanin,[1,2] I. V. Kukushkin,[1] L. Tiemann,[3] C. Reichl,[3] W. Dietsche,[3] and W. Wegscheider[3]

[1]*Institute of Solid State Physics RAS, Chernogolovka 142432, Russia*

[2]*Moscow Institute of Physics and Technology, Dolgoprudny 141700, Russia*

[3]*Solid State Physics Laboratory, ETH Zurich, Schafmattstrasse 16, 8093 Zurich, Switzerland*

(Received 27 May 2015; published 15 July 2015)

The spectra of plasma and magnetoplasma excitations in a two-dimensional system of anisotropic heavy fermions are investigated. The spectrum of microwave absorption by disklike samples of stressed AlAs quantum wells at low electron densities shows two plasma resonances separated by a frequency gap. These two plasma resonances correspond to electron mass principle values of $(1.10 \pm 0.05)m_0$ and $(0.20 \pm 0.01)m_0$. The observed results correspond to the case of a single valley strongly anisotropic Fermi surface. It is established that an increase in electron density results in the population of the second valley, manifesting itself as a drastic modification of the plasma spectrum. We directly determine the electron densities in each valley and the intervalley splitting energy from the ratio of the two plasma frequencies.

DOI: 10.1103/PhysRevB.92.041303 PACS number(s): 73.63.Hs, 72.30.+q, 73.50.Mx, 73.20.Mf

The last few decades have witnessed a surge in research on the fascinating and often unexpected collective states arising from strong electron-electron interactions. Selectively doped semiconductor heterostructures appeared to be nearly ideal systems for such research owing to their strongly reduced disorder. Examples of phenomena caused by electron correlations include the fractional quantum Hall effect [1], metal-insulator transitions [2], and spin-textured structures [3]. The electron-electron interaction strength is characterized by the ratio of the Coulomb interaction energy to the Fermi energy, and is proportional to the effective mass of charge carriers. This has motivated interest in new two-dimensional electron systems (2DESs) that show heavy fermion behavior. One of the most promising materials of choice is n-AlAs [4].

AlAs is an indirect gap semiconductor in which the electrons occupy three equivalent valleys at the X points of the Brillouin zone. This degeneracy is lifted when the electrons are confined to a 2D layer. In a quantum well grown on a GaAs (001) wafer, only the in-plane [100] (X) and [010] (Y) valleys are occupied for well widths greater than 5 nm [5]. This differs from Si (001) metal-oxide-semiconductor field-effect transistors (MOSFETs), in which the two valleys with out-of-plane major axes are occupied. Such unusual behavior stems from the biaxial compression of the AlAs layer, induced by a lattice mismatch between the AlAs and GaAs. Moreover, the residual in-plane strain lifts the X and Y valley degeneracy, leading to intervalley energy splitting ΔE (Fig. 1) [6–9]. This splitting modifies the plasma spectrum, as observed in the present Rapid Communication. Transport measurements revealed large and anisotropic AlAs electron effective masses $m_l = (1.1 \pm 0.1)m_0$ and $m_{tr} = (0.20 \pm 0.02)m_0$ [10–12], corresponding to the longitudinal and transverse Fermi ellipsoid axis directions, respectively. The effective Landé g factor of electrons in bulk AlAs ($g^* = 2$) is much larger than in GaAs ($g^* = -0.44$). These characteristics make the AlAs heterostructure 2DES a unique and versatile subject of many-body and valleytronics phenomena investigations.

Microwave magnetospectroscopy is the most direct method to characterize Fermi surfaces and determine effective masses [13]. This method has revealed well-studied 2D plasma excitations in an isotropic single component GaAs heterostructure 2DES [14,15]. Attempts to study plasma dynamics in an anisotropic 2DES, however, have been limited to experiments in which an applied magnetic field creates a small anisotropy in an initially isotropic 2DES [16–18]. An example of collective behavior in a multicomponent 2DES was found in GaAs double quantum wells occupied by electrons in one well and holes in the other [19]. Heretofore, 2D-plasmon physics in systems with native strong mass anisotropy, as well as multicomponent 2DESs, has not been well explored, despite a number of interesting physical predictions [20]. The AlAs 2DES provides an important research opportunity by combining strong anisotropy with the ability to tune the carrier density in each valley.

Measurements were carried out on high-quality 15 nm AlAs quantum well heterostructures fabricated by molecular beam epitaxy (MBE) on a (001) GaAs substrate. The electron density n_s and electron mobility μ were in the ranges of $(1.7\text{–}2.4) \times 10^{11}$ cm^{-2} and $(1.2\text{–}2.0) \times 10^5$ cm^2/V s, respectively. A variation of the electron density was achieved by short illumination of the sample. The illumination was performed by a green light emitting diode (2.2 eV) at $T = 1.6$ K. A coplanar waveguide (CPW) was fabricated on top of the crystal surface using standard photolithography tools. The waveguide contained a central 1.1 mm wide stripe spaced 0.6 mm from the grounded planes (see the inset in Fig. 1). The total length of the coplanar waveguide was 4 mm. The parameters of the waveguide were chosen to provide a characteristic impedance of $Z_0 = 50\ \Omega$. Six equidistant 2DES disks of diameter $d = 0.5$ mm were fabricated in the slots of the CPW. The disk centers were spaced 1.5 mm apart to minimize crosstalk effects. Arrows indicate the basic crystallography directions in Fig. 1. We detected the resonant absorption of microwave probe radiation ($f =$ 1–40 GHz) propagating along the CPW. An alternating electric field concentrated in the slots of the CPW oscillates the 2D plasmas in the disks. The resonant absorption of microwaves occurs whenever a plasmon is excited in a disk. The sample was immersed in a cryostat with a superconducting coil. Here, 50 Ω coaxial cables connected the sample in a series between a microwave generator ($f =$ 0–40 GHz) and a tunnel diode with

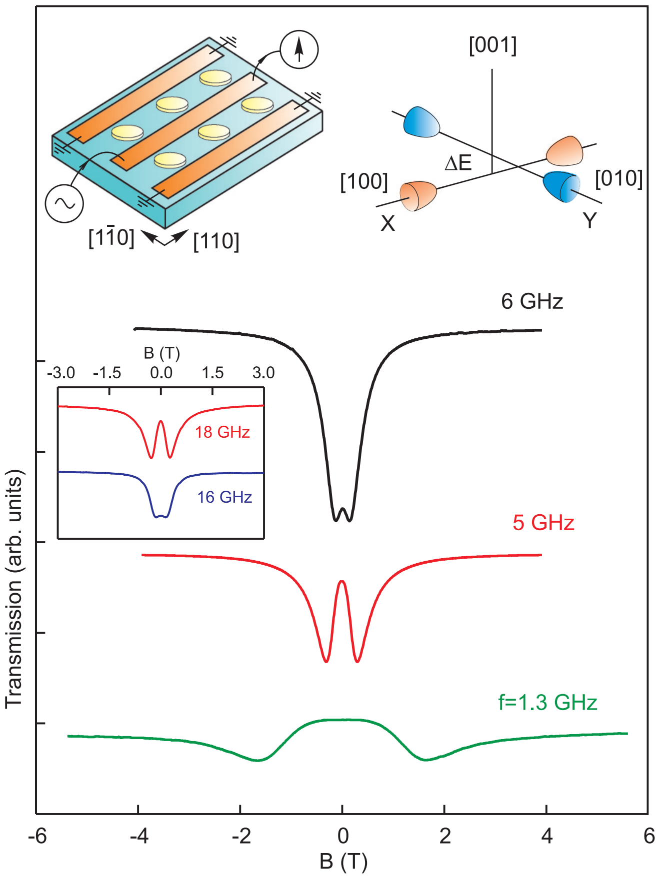

FIG. 1. (Color online) Magnetic-field dependencies of the coplanar waveguide transmission at microwave frequencies of 1.3, 5, and 6 GHz. Each curve shows a well-defined resonance corresponding to edge magnetoplasmon excitation. Residual in-plane strain in a semiconductor structure causes a rise of the energy gap ΔE between the X and Y valleys. The inset shows CPW transmission at 16 and 18 GHz. The resonances exhibit positive magnetodispersion inherent to a cyclotron magnetoplasmon. The electron density is $n_s = 1.7 \times 10^{11}$ cm^{-2} at $T = 1.5$ K. Schematic drawings of the coplanar waveguide indicating the basic crystallography directions and the AlAs Fermi surface are shown in the upper left and right, respectively.

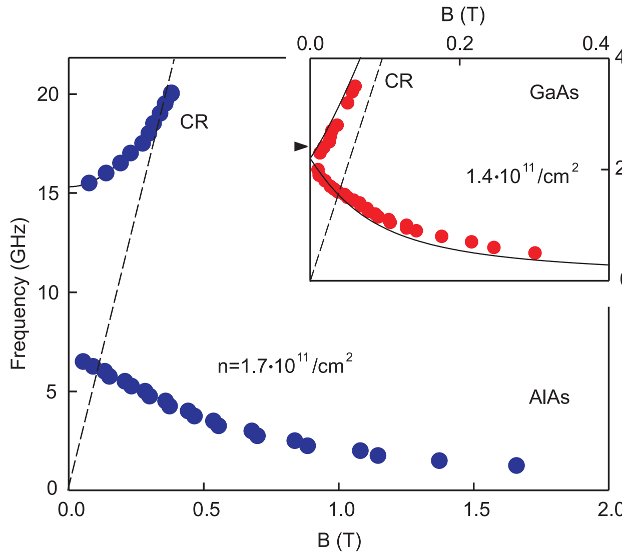

FIG. 2. (Color online) Magnetodispersion of two-dimensional plasma excitations in AlAs disks with anisotropic charge carriers ($n_s = 1.7 \times 10^{11}$ cm^{-2}). The plasmon spectrum shows two plasma resonance branches separated by a frequency gap. The inset shows the dispersion of magnetoplasmon waves in a GaAs quantum well for electrons with isotropic mass ($n_s = 1.4 \times 10^{11}$ cm^{-2}). No frequency gap is observed. The same disk and CPW geometry were used in both cases.

a preamplifier placed outside the cryostat. The output power of the generator did not exceed 100 nW and the output signal was detected by a standard lock-in technique. The magnetic field was applied normal to the surface of the sample. Helium vapor was pumped out to attain a temperature of $T = 1.6$ K.

Figure 1 shows the magnetic-field dependencies of the coplanar waveguide transmission for several microwave frequencies. The horizontal axis is located at the signal level when no microwave radiation is supplied to the CPW. Each curve shows a resonance with respect to zero magnetic field. Most of the resonances are symmetric, and the rest have an asymmetric line shape. The observed asymmetric resonances in the transmission can be treated and analyzed as Fano-type resonances (see Ref. [21] and the Supplemental Material [22]). The resonance shifts to lower magnetic fields with increasing microwave frequency f, indicating the edge magnetoplasma (EMP) nature of the observed resonance. For frequencies above 15 GHz, a second plasma resonance arises (see the inset in Fig. 1). The resonance behavior exhibits a positive magnetodispersion characteristic of the cyclotron magnetoplasmon. For more transmission curves, we refer to Fig. S1 in the Supplemental Material [22].

The resonance origins are best identified by plotting the resonant magnetic field versus microwave frequencies, as shown in Fig. 2. The data were obtained at an electron density of 1.7×10^{11} cm^{-2}. The magnetodispersion has two branches separated by a frequency gap. The low-frequency branch corresponds to an edge magnetoplasmon propagating along the edge of the disk. This is a mode with anomalously weak attenuation that propagates in a narrow strip near the edge of the 2DES [23,24]. The EMP frequency decreases as $\omega_- \approx \sigma_{xy} q \propto n_s q / B$ in the strong magnetic-field limit. The high-frequency branch has a positive magnetodispersion. The electric field $\vec{E}$ aligned along the [1$\bar{1}$0] (Fig. 1) crystal direction can be factorized into two components along the Fermi ellipsoid axes as $\vec{E} = \vec{E}_l + \vec{E}_{tr}$. In the $B = 0$ T limit, each of these components excites a separate 2D plasma wave with corresponding masses m_l and m_{tr}. Therefore, the gap in the magnetoplasmon spectrum of the disk vividly demonstrates the highly anisotropic nature of the Fermi surface in AlAs 2DESs [18,25]. For the sake of comparison, we performed the same measurements on a geometrically identical sample made from a GaAs quantum well ($d = 0.5$ mm, $n_s = 1.4 \times 10^{11}$ cm^{-2}). The inset in Fig. 2 shows that for $B = 0$ T, the magnetic field edge and cyclotron magnetoplasma modes are degenerate, highlighting the mass $m^* = 0.067 m_0$ isotropism in GaAs.

The plasma excitation spectrum in a 2DES with mass anisotropy can be described using the dipole approximation as [25–27]

$$\omega_{\mathrm{l,tr}} = \tfrac{1}{2}\Big[\sqrt{(\Omega_{\mathrm{tr}}+\Omega_{\mathrm{l}})^2+\omega_c^2} \pm \sqrt{(\Omega_{\mathrm{tr}}-\Omega_{\mathrm{l}})^2+\omega_c^2}\Big], \quad (1)$$

where Ω_{l} and Ω_{tr} are plasma frequencies along the main crystallographic directions for $B = 0$ T, and $\omega_c = eB/m_c$ is the cyclotron frequency. The cyclotron mass is determined as a geometric mean of effective masses along the crystallographic axes, $m_c = \sqrt{m_{\mathrm{l}} m_{\mathrm{tr}}}$. The frequencies $\Omega_{\mathrm{l,tr}}$ obey the 2D-plasmon dispersion [14]

$$\Omega^2_{\mathrm{l,tr}} = \frac{n_s e^2}{2 m_{\mathrm{l,tr}} \varepsilon_0 \varepsilon^*} q, \quad (2)$$

where $\varepsilon^* = (\varepsilon_{\mathrm{GaAs}} + 1)/2$ is the effective dielectric permittivity of the surrounding medium and $q = 2.4/d$ is the wave vector for the disk geometry [28]. From our experiments, we measure zero-field plasma frequencies $\Omega_{\mathrm{l}} = (6.5 \pm 0.2)$ GHz and $\Omega_{\mathrm{tr}} = (15.3 \pm 0.5)$ GHz. Using Eq. (2) we find the effective masses in the AlAs quantum well along the main crystallographic directions to be $m_{\mathrm{l}} = (1.10 \pm 0.05) m_0$ and $m_{\mathrm{tr}} = (0.20 \pm 0.01) m_0$. These mass values agree with results obtained from commensurability oscillation measurements [4].

Figure 3(a) shows CPW microwave transmission as a function of magnetic field for identical samples with 2DES densities of 1.7×10^{11} and 2.4×10^{11} cm^{-2}. A short light flash from a light emitting diode varied the electron density. The magnetoplasma resonance shifted to larger magnetic-field values with increased electron density. This is consistent with Eqs. (1) and (2). However, the zero-field plasma frequencies determined from the detailed magnetodispersion curve of the 2.4×10^{11} cm^{-2} 2DES have a ratio $\Omega_{\mathrm{tr}}/\Omega_{\mathrm{l}} = (1.80 \pm 0.05)$. This number is inconsistent with Eq. (2), which predicts $\Omega_{\mathrm{tr}}/\Omega_{\mathrm{l}} = \sqrt{m_{\mathrm{l}}/m_{\mathrm{tr}}} = (2.3 \pm 0.1)$. This suggests that the plasma dynamics undergoes a qualitative metamorphosis when the electron density changes.

We attribute the observed phenomenon to the energy splitting between the X and Y valleys. Indeed, the residual in-plane strain lifts the X and Y valley degeneracy, leading to an intervalley energy splitting ΔE (Fig. 1). For a 2DES where $n_s = 1.7 \times 10^{11}$ cm^{-2}, we find that all electrons occupy only the X valley, leaving the Y valley empty. As we increase the density, some of the electrons begin to fill the Y valley [Fig. 3(b)]. The total density is then defined as $n_s = n_x + n_y$, where n_x and n_y are the charge carrier concentrations in the X and Y valleys, respectively. The collective plasma excitations in such a system could be considered using a two-component anisotropic plasma model [29]. The plasma frequencies along the [100] and [010] directions are described by the following expressions:

$$\Omega^2_{[100]} = \frac{e^2 q}{2\varepsilon_0 \varepsilon^*}\left(\frac{n_x}{m_{\mathrm{l}}} + \frac{n_y}{m_{\mathrm{tr}}}\right), \quad (3)$$

$$\Omega^2_{[010]} = \frac{e^2 q}{2\varepsilon_0 \varepsilon^*}\left(\frac{n_x}{m_{\mathrm{tr}}} + \frac{n_y}{m_{\mathrm{l}}}\right). \quad (4)$$

Using these expressions with our obtained plasma frequencies $\Omega_{[100]}, \Omega_{[010]}$ and AlAs masses $m_{\mathrm{l}}, m_{\mathrm{tr}}$, we deduced the densities n_x and n_y in each of the valleys to be $n_x = (2.10 \pm 0.05) \times 10^{11}$ cm^{-2} and $n_y = (0.30 \pm 0.05) \times$

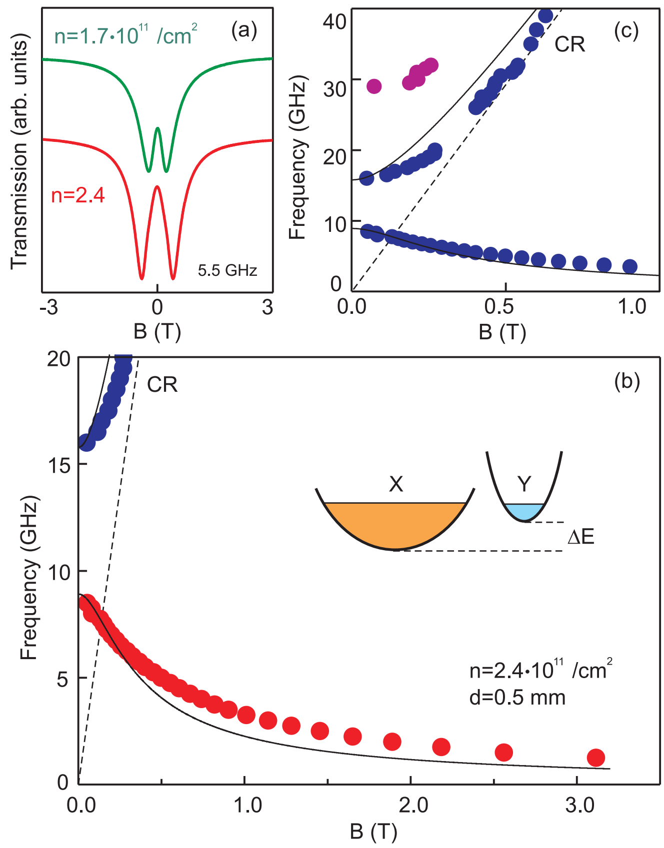

FIG. 3. (Color online) (a) Magnetic-field dependencies of the coplanar waveguide transmission for microwave frequency $f = 5.5$ GHz with two different 2DES densities. (b) Dispersion of two-dimensional magnetoplasma excitations in an AlAs quantum well at $n_s = 2.4 \times 10^{11}$ cm^{-2}. The solid line represents the theoretical prediction according to Eq. (1). Schematic drawing of the electron spectrum for $n_s = 2.4 \times 10^{11}$ cm^{-2}. The Y valley starts to be filled at this density. (c) Extended magnetodispersion of the plasmon modes.

10^{11} cm^{-2}. From the difference of densities $\Delta n = n_x - n_y$, we can directly determine the intervalley energy splitting ΔE using the 2D density of states:

$$\Delta E = \frac{\pi \hbar^2 \Delta n}{\sqrt{m_{\mathrm{l}} m_{\mathrm{tr}}}}. \quad (5)$$

This calculation gives $\Delta E = (0.90 \pm 0.05)$ meV, which is consistent with all previous studies of valley splitting in AlAs [6–8]. However, these studies were conducted in strong magnetic fields ($B > 1$ T), leaving the low magnetic field range unexplored. Our experiments directly determine the valley populations from the plasma frequencies in the weak magnetic field limit.

The solid lines in Figs. 3(b) and 3(c) represent the theoretical predictions of Eq. (1) with $\Omega_{\mathrm{l}} = \Omega_{[100]}$ and $\Omega_{\mathrm{tr}} = \Omega_{[010]}$ for the mode magnetodispersion. Some discrepancy exists between the experimental data and theory at moderate magnetic fields. The difference is especially pronounced for the high-frequency cyclotron magnetoplasma mode [Fig. 3(c)]. One possible explanation could be the hybridization between the cyclotron magnetoplasma mode and an intercomponent cyclotron mode. The additional intercomponent mode is a dispersionless excitation with frequency $\omega = eB/\sqrt{m_l m_{tr}}$, which coincides with the cyclotron resonance [20]. Another possible explanation of the observed discrepancy is that $\Omega_{[100]}$, $\Omega_{[010]}$, and the corresponding ΔE are not constant with the B field. This discrepancy should motivate further research. The agreement between theory and experiment returns in the limit of strong magnetic fields.

Our results suggest opportunities for future applications of plasmonics in AlAs 2DESs. They can be used to study the intervalley energy spacing at $B = 0$ T using the discovered plasma resonance method. Such experiments could unveil the roles of electron-electron interactions in semiconductor valley splitting [6–8]. They could also be used to study relativistic plasma excitations [30]. Relativistic plasma waves in highly anisotropic two-component electron liquids of AlAs may reveal unpredicted physical phenomena.

The authors gratefully acknowledge financial support from the Russian Scientific Fund (Grant No. 14-12-00693).

[1] D. C. Tsui, H. L. Stormer, and A. C. Gossard, Phys. Rev. Lett. **48**, 1559 (1982).
[2] S. V. Kravchenko, G. V. Kravchenko, J. E. Furneaux, V. M. Pudalov, and M. D'Iorio, Phys. Rev. B **50**, 8039 (1994).
[3] X. Z. Yu, Y. Onose, N. Kanazawa, J. H. Park, J. H. Han, Y. Matsui, N. Nagaosa, and Y. Tokura, Nature **465**, 901 (2010).
[4] M. Shayegan, E. P. De Poortere, O. Gunawan, Y. P. Shkolnikov, E. Tutuc, and K. Vakili, Phys. Status Solidi B **243**, 3629 (2006).
[5] K. Maezawa, T. Mizutani, and S. Yamada, J. Appl. Phys. **71**, 296 (1992).
[6] T. Ando, A. B. Fowler, and F. Stern, Rev. Mod. Phys. **54**, 437 (1982).
[7] Y. P. Shkolnikov, E. P. De Poortere, E. Tutuc, and M. Shayegan, Phys. Rev. Lett. **89**, 226805 (2002).
[8] Y. P. Shkolnikov, S. Misra, N. C. Bishop, E. P. De Poortere, and M. Shayegan, Phys. Rev. Lett. **95**, 066809 (2005).
[9] S. Prabhu-Gaunkar, S. Birner, S. Dasgupta, C. Knaak, and M. Grayson, Phys. Rev. B **84**, 125319 (2011).
[10] T. P. Smith, III, W. I. Wang, F. F. Fang, and L. L. Chang, Phys. Rev. B **35**, 9349(R) (1987).
[11] T. S. Lay, J. J. Heremans, Y. W. Suen, M. B. Santos, K. Hirakawa, M. Shayegan, and A. Zrenner, Appl. Phys. Lett. **62**, 3120 (1993).
[12] O. Gunawan, Y. P. Shkolnikov, E. P. De Poortere, E. Tutuc, and M. Shayegan, Phys. Rev. Lett. **93**, 246603 (2004).
[13] G. Dresselhaus, A. F. Kip, and C. Kittel, Phys. Rev. **98**, 368 (1955).
[14] Frank Stern, Phys. Rev. Lett. **18**, 546 (1967).
[15] S. J. Allen, Jr., D. C. Tsui, and R. A. Logan, Phys. Rev. Lett. **38**, 980 (1977).
[16] E. Batke and C. W. Tu, Phys. Rev. B **34**, 3027(R) (1986).
[17] V. E. Kozlov, S. I. Gubarev, I..V. Kukushkin, JETP Lett. **94**, 397 (2011).
[18] V. E. Kozlov, S. I. Gubarev, A. A. Dremin, I. V. Kukushkin, JETP Lett. **96**, 525 (2012).
[19] I. V. Kukushkin, A. V. Rossokhaty, S. Schmult, and K. von Klitzing, Semicond. Sci. Technol. **26**, 014023 (2011).
[20] A. V. Chaplik, Surf. Sci. Rep. **5**, 289 (1985).
[21] Ugo Fano, Phys. Rev. **124**, 1866 (1961).
[22] See Supplemental Material at http://link.aps.org/supplemental/10.1103/PhysRevB.92.041303 for additional pictures of edge magnetoplasma resonance and analysis of the resonance lineshape.
[23] V. A. Volkov and S. A. Mikhailov, Zh. Eksp. Teor. Fiz. **94**, 217 (1988) [Sov. Phys. JETP Lett. **67**, 1639 (1988)].
[24] S. J. Allen, Jr., H. L. Störmer, and J. C. M. Hwang, Phys. Rev. B **28**, 4875(R) (1983).
[25] C. Dahl, F. Brinkop, A. Wixforth, J. P. Kotthaus, J. H. English, and M. Sundaram, Solid State Commun. **80**, 673 (1991).
[26] V. Shikin, S. Nazin, D. Heitmann, and T. Demel, Phys. Rev. B **43**, 11903 (1991).
[27] V. A. Geyler, V. A. Margulis, and A. V. Shorokhov, Phys. Rev. B **63**, 245316 (2001).
[28] I. V. Kukushkin, J. H. Smet, S. A. Mikhailov, D. V. Kulakovskii, K. von Klitzing, and W. Wegscheider, Phys. Rev. Lett. **90**, 156801 (2003).
[29] R. Z. Vitlina and A. V. Chaplik, Sov. Phys. JETP **54**, 536 (1981).
[30] V. M. Muravev, P. A. Gusikhin, I. V. Andreev, and I. V. Kukushkin, Phys. Rev. Lett. **114**, 106805 (2015).